Optimal Design of Truss Structures by Rescaled Simulated Annealing

Jungsun Park*, Miran Ryu
School of Aerospace and Mechanical Engineering, Hankuk Aviation University, 200-1, Hwajon-dong, Deokyang-gu, Koyang-si, Kyonggi-do, 412-791, Korea

Rescaled Simulated Annealing (RSA) has been adapted to solve combinatorial optimization problems in which the available computational resources are limited. Simulated Annealing (SA) is one of the most popular combinatorial optimization algorithms because of its convenience of use and because of the good asymptotic results of convergence to optimal solutions. However, SA is too slow to converge in many problems. RSA was introduced by extending the Metropolis procedure in SA. The extension rescales the state's energy candidate for a transition before applying the Metropolis criterion. The rescaling process accelerates convergence to the optimal solutions by reducing transitions from high energy local minima. In this paper, structural optimization examples using RSA are provided. Truss structures of which design variables are discrete or continuous are optimized with stress and displacement constraints. The optimization results by RSA are compared with the results from classical SA. The comparison shows that the numbers of optimization iterations can be effectively reduced using RSA.

Key Words : Optimization, Rescaled Simulated Annealing, Truss Structure

1. Introduction

The gradient-based optimization techniques (Rao, 1996) are classical optimization methods. The gradient information in the classical optimization methods is very difficult to find in many structural design problems. The classical optimization methods are not suitable to the optimization with discrete design variables because the discrete optimization functions are not differentiable. The classical optimization methods may provide several local optimum values to multiple local optimum problems. Therefore, Simulated Annealing (Aarts and Kost, 1989), a stochastic search algorithm with randomized variables, is used to overcome the gradient limitations in the classical gradient-based optimization methods.

The concept behind the Simulated Annealing algorithm was derived from statistical mechanics and motivated by an analogy to the behavior of physical annealing. Simulated Annealing has been applied to the traveling salesman problem, which is a typical example of combinatorial optimization problems (Gelatt et al., 1983; Černy, 1985). The Simulated Annealing algorithm has been extensively described for general applications (Aarts and Laarhoven, 1987). A multi-objective constrained truss structure has been optimized for weight, displacement and natural frequency (Bennage and Dhingra, 1995). The Simulated Annealing algorithm has been applied to a three-dimensional, six-story, unsymmetrical steel frame (Balling, 1991). Topology optimization for maximum natural frequency was performed by Cui, Tai and Wang (2000). Distortion and internal forces in truss structures have been minimized by Kincaid and Padula (1990).

* Corresponding Author,
E-mail : jungsun@mail.hangkong.ac.kr
TEL : +82-2-300-0283; **FAX** : +82-2-3158-3189
School of Aerospace and Mechanical Engineering, Hankuk Aviation University, 200-1, Hwajon-dong, Deokyang-gu, Koyang-si, Kyonggi-do, 412-791, Korea. (Manuscript **Received** July 16, 2003; **Revised** June 28, 2004)

However, SA is slow to converge to an optimal value. For improving convergence speed, Lundy et al. have suggested a more elaborate cooling schedule (Lundy, 1986). Parallel Simulated Annealing algorithms have been suggested for several applications (Aarts and Kost, 1989). Adaptive Simulated Annealing (ASA) has been proposed for practical optimization (Ingber, 1995). For faster convergence, new algorithms have been developed to devise the necessary cooling schedules. On the other hand, Rescaled Simulated Annealing does not use the cooling schedule. To reduce computational effort, RSA has been utilized by manipulating the cooling schedule (Herault, 2000).

The concept of the RSA algorithm is the generalization of the Metropolis criterion in SA, which decides whether the current energy state is accepted or whether to go to the next state. Instead of going to a low energy (objective function) state, it allots energy around the target energy at each temperature step. The target energy varies with temperature change. As numerical examples of the Rescaled Simulated Annealing algorithm, truss structures are optimized. The optimum results and the numbers of function evaluations by the Rescaled Simulated Annealing algorithm are compared to those by the conventional Simulated Annealing algorithm.

2. Rescaled Simulated Annealing

The Rescaled Simulated Annealing algorithm (RSA) is derived from the physical annealing process that is performed in order to obtain the minimum (ground) energy state. The ground state is obtained only if the temperature (design variable) of the heat bath is increased to the maximum value at which solid melts and is decreased very slowly until the particles arrange themselves in the ground state of the solid. In the ground state the particles are arranged structurally and the energy of the system is minimal (meta-stable state). Thermodynamics of the annealing process can be expressed as the Boltzmann Probability Distribution. The Boltzmann Probability Distribution (Aart and Kost, 1989) of the solid in state i with energy E_i at temperature T can be written as Eq. (1).

$$P_T\{X=i\}=\frac{1}{Z(T)}\exp\left(\frac{-E_i}{k_BT}\right) \tag{1}$$

where X is a stochastic variable.

$Z(T)$ is the partition function.

$$Z(T)=\sum_j \exp\left(\frac{-E_j}{k_BT}\right) \tag{2}$$

During the physical annealing process, the minimum energy state corresponds to the minimum objective function in RSA. Acceptance criterion (Metropolis criterion) of Rescaled Simulated Annealing determines whether or not the next state is accepted from the current state by applying the following acceptance probability (Aart and Laarhoven, 1987)

$$A_{ij}(c)=\begin{cases} 1 & \text{if } \Delta E_{ij}\le 0 \\ \exp\left(\dfrac{-\Delta E_{ij}}{c}\right) & \text{if } \Delta E_{ij}>0 \end{cases} \tag{3}$$

$$\Delta E_{ij}=(\sqrt{E_j}-\sqrt{E_{target}})^2-(\sqrt{E_i}-\sqrt{E_{target}})^2 \tag{4}$$

$$E_{target}=a\cdot c^2 \tag{5}$$

where c is the control parameter (temperature parameter) and parameter a is experimentally determined from the initial temperature step.

If the objective function of current state i is larger than that of the next state j, the next state will be accepted. Otherwise, a random number is generated between 0 and 1. The generated random number is compared with the acceptance probability. When the acceptance probability is larger than the random number, the next state instead of the current state is accepted to escape the local optimum.

To illustrate the rescaling of the energy, an example of one-dimensional functions in Eq. (6), is shown in Fig. 1. The deformation of the energy landscape of Eq. (7) is shown in Fig. 2. as a function of the target energy. If the target energy is zero, the rescaled energy is the original one.

$$F(x)=(8+|1.5-x|\times\sin(2\times x)/x) \tag{6}$$

$$F(x, E_{target})=(\sqrt{8+|1.5-x|\times\sin(2\times x)/x}-\sqrt{E_{target}})^2 \tag{7}$$

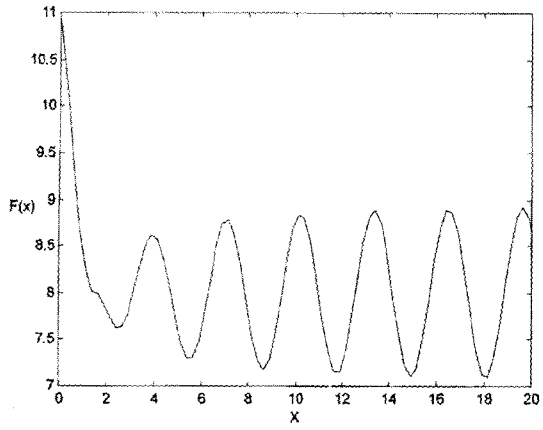

Fig. 1 Example of a 1-D function

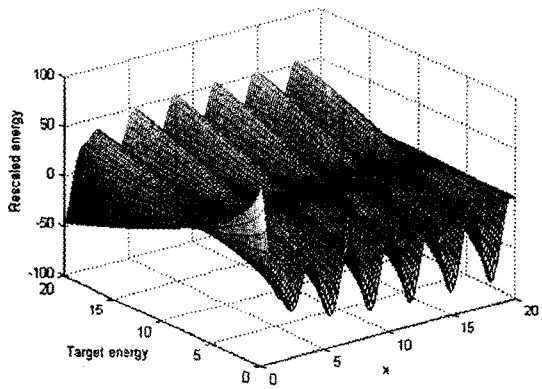

Fig. 2 Example of rescaled energy

At high target energies, the minimum values of the rescaled energy correspond to the maximum values of the original one. If the target energy is lower than the original energy, the minimum values of the rescaled energy correspond to the minimum values of the original energy. As the target energy is reduced, the rescaled energy is converged toward the original one. More precisely, when the target energy becomes smaller than the least energy, the minimum values of the rescaled energy landscape are also minimum values in the original energy landscape. Therefore, the optimal states of the problems with rescaled energies are also optimal in the original energy landscape. Furthermore, the local minimum values of the rescaled energy landscape are shallower than in the original landscape. For convergence of the rescaled energy, the target energy is set lower than the original energy. The parameter a was chosen so that the initial target energy is near the mean energy of the states.

During the annealing process, after $N \times NS \times NT$ function evaluations, temperature is changed by the following Eq. (8)

$$T(i+1) = RT \times T(i) \tag{8}$$

where RT is the temperature reduction factor, N is the number of design variables, NS is the number of cycles (temperature changes) and NT indicates the number of iterations before temperature changes. After $N \times NS$ function evaluations, each element of step length vector, which is related to the neighborhood of design variables, is adjusted.

Rescaled Simulated Annealing is terminated when the number of function evaluations is greater than the maximum evaluation or the temperature is sufficiently low. In this study, for the termination of numerical iterations, the small error tolerance (EPS) is taken. The maximum evaluation is set very large to avoid being terminated before optimum. Error tolerance is defined as

$$F(X_{i+1}) - F(X_i) \leq EPS \tag{9}$$

In this study, EPS is set to 10^{-3} and NEPS (number of final function values) to 4, which is used to decide termination. The flowchart of Rescaled Simulated Annealing is shown in Fig. 3.

Rescaled Simulated Annealing is an originally unconstrained optimization method. The unconstrained optimization problems are changed to constrained optimization problems by introducing the penalty function. The penalty function imposes a penalty to a pseudo-objective function (10) considering the constraint violation

$$P = F(X) + \sum_{i=1}^{m} R_i \Phi(g_j(X)) \tag{10}$$

$$\Phi(g_j(X)) = \langle g_j(X) \rangle^2 \tag{11}$$

$$\langle g_j(X) \rangle = \begin{cases} g_j(X) & \text{if } g_j(X) > 0 \\ 0 & \text{if } g_j(X) \leq 0 \end{cases} \tag{12}$$

where F is objective function, Φ is penalty function, $g_j(X)$ are constraints, and m is the number of constraints.

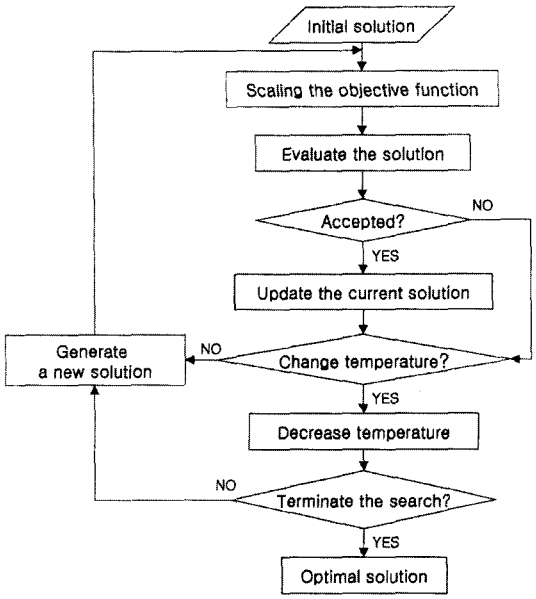

Fig. 3 Flowchart of the RSA

3. Optimization of Truss Structure by RSA

Truss structures are presented for the structural optimization examples using RSA. The objective functions are the weights of the structures. The design variables are the cross sectional areas of truss members. The constraints are imposed on the allowable stresses of the truss members and the maximum allowable displacements at the joints. The objective function and the constraints are expressed by the following equations

$$\text{Minimize}: F=\sum_{i=1}^{n}\rho A_i l_i \tag{13}$$

$$\text{Subject to}: \frac{\sigma_i}{\sigma_{ia}}-1\leq 0 \qquad i=1, \cdots, n_t \tag{14}$$

$$\frac{w_j}{w_{\max}}-1\leq 0 \qquad j=1, \cdots, n_d \tag{15}$$

where n means the number of design variables A_i, n_t the number of truss members and n_d the number of nodes with displacements constraints.

3.1 Ten-bar truss

The ten-bar truss shown in Fig. 4 is optimized for both continuous and discrete design

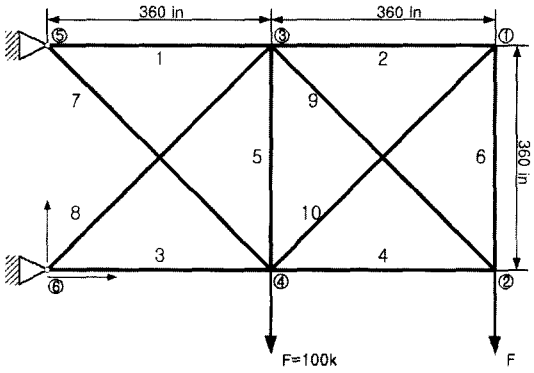

Fig. 4 Ten bar truss

variables, respectively. The same stress and displacement constraints are imposed on the continuous and discrete problems. The allowable stress $\sigma_a=25000psi$ is applied for all members. The maximum allowable displacement $w_{\max}=\pm 2in$ is applied for nodal displacements in x- and y-directions. For all members, the same weight density ($\rho=0.01lb/in^3$), and Young's modulus (10^7psi) are used. In the discrete design variable problems, candidate cross sectional areas are the following 42 discrete design variables used by Bennage and Dhingra (1995).

[1.62, 1.8, 1.99, 2.13, 2.38, 2.62, 2.63, 2.88, 2.93, 3.09, 3.13, 3.38, 3.47, 3.55, 3.63, 3.84, 3.87, 3.88, 4.18, 4.22, 4.49, 4.59, 4.80, 4.97, 5.12, 5.74, 7.22, 7.97, 11.5, 13.5, 13.9, 14.2, 15.5, 16.0, 16.9, 18.8, 19.9, 22.0, 22.9, 26.5, 30.0, 33.5] in^2

The continuous and discrete optimization results from RSA and SA are shown in Table 1~2. The optimization results from the classical gradient based method are added in Table 1 for verification of the present work. As shown in Table 1, the optimal weights of RSA and SA are close to those of the gradient based optimization method (Haug and Arora, 1979). The number of function evaluations in the optimization using RSA is reduced 19.54% in continuous variable optimization, and 11.27% in discrete variable optimization in comparison to SA. In the continuous optimization shown in Table 1, the optimal weight from RSA is 6.7% less than the optimal weight from SA. In the discrete optimization shown in Table 2, the optimal weight

from RSA is 3.0% less than the optimal weight from SA. The optimization by RSA requires a smaller number of iterations and produces a better quality of optimization results in comparison to SA.

Table 1 10-bar truss optimization results with continuous variables (in^2)

	Initial Design	RSA	SA	Haug*
A_1	33.5	28.23	28.2	30.03
A_2	10.0	0.10	2.83	0.10
A_3	30.0	23.01	30.06	23.27
A_4	30.0	12.78	13.37	15.28
A_5	10.0	0.10	0.10	0.10
A_6	10.0	0.10	1.86	0.55
A_7	20.0	8.86	13.14	7.46
A_8	20.0	25.39	21.08	21.19
A_9	30.0	21.02	17.77	21.61
A_{10}	10.0	0.10	2.39	0.10
Objective function (lb)	8518.94	5136.12	5482.88	5051.60
Number of function evaluations		4160	5170	NA

*Results from Haug and Arora (1979)

Table 2 10-bat truss optimization results with discrete variables (in^2)

	Initial Design	RSA	SA
A_1	33.5	33.5	22.0
A_2	10.0	1.62	2.62
A_3	30.0	22.0	26.5
A_4	30.0	11.5	14.2
A_5	10.0	1.62	1.62
A_6	10.0	1.99	2.63
A_7	20.0	14.2	16.0
A_8	20.0	20.0	19.9
A_9	30.0	22.9	26.5
A_{10}	10.0	3.63	3.55
Objective function (lb)	8518.94	5692.15	5862.15
Number of function evaluations		2440	2750

3.2 Twenty- five bar truss

A twenty-five bar truss structure is shown in Fig. 5. The allowable stress $\sigma_a=40000psi$ is applied to all members. The maximum allowable displacements $w_{max}=\pm 0.35in$ is applied for nodal displacement in the x and y directions. The loadings are applied as shown in Table 3. Design variables of the twenty-five bar truss structure are cross sectional areas. The twenty-five bar truss structure is symmetric with respect to the Y-Z axis. Design variables of the truss structure are reduced by symmetry. The relationship of cross sectional areas and design variables is shown in Table 4. Similar to the ten-bar truss, the twenty five-bar truss structure is optimized for both continuous and discrete variables, respectively. In the discrete variable optimization, candidate cross sectional areas are $[0.1i(i=1, \cdots, 26), 2.8, 3.0, 3.2, 3.4]in^2$. The optimization results of the 25-bar truss structure are shown in Table 5~6. The 25-bar truss

Table 3 Loading conditions

Joint	$F_x(lb)$	$F_y(lb)$	$F_z(lb)$
1	1000	10000	−10000
2	0	10000	−10000
3	500	0	0
6	600	0	0

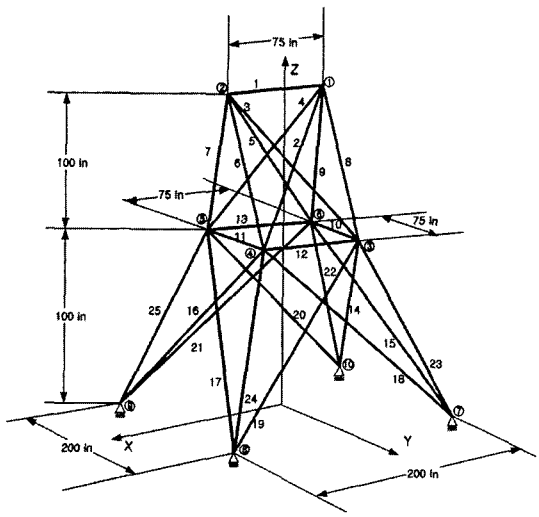

Fig. 5 Twenty-five bar truss

Table 4 Relationship between design variables and truss members

Design variables	Truss members
1	1
2	2, 3, 4, 5
3	6, 7, 8, 9
4	10, 11
5	12, 13
6	14, 15, 16, 17
7	18, 19, 20, 21
8	22, 23, 24, 25

Table 5 25-bar truss optimization results with continuous variables (in^2)

	Initial Design	RSA	SA	Haug*
A_1	1.0	0.10	0.10	0.01
A_2	3.4	0.14	0.46	2.04
A_3	3.4	3.34	3.35	2.99
A_4	1.0	0.10	0.10	0.01
A_5	3.4	0.89	0.54	0.01
A_6	2.0	0.99	0.75	0.68
A_7	3.4	1.5	1.93	1.62
A_8	3.4	3.04	2.81	2.67
Objective function (lb)	969.0108	507.14	522.16	545.04
Number of function evaluations		9200	11350	NA

* Results from Haug and Arora (1979)

Table 6 25 bar truss optimization results with discrete variables (in^2)

	Initial Design	RSA	SA
A_1	1.0	0.3	0.2
A_2	3.4	2.8	3.2
A_3	3.4	2.1	1.6
A_4	1.0	0.2	0.2
A_5	3.4	0.3	0.5
A_6	2.0	0.8	1.1
A_7	3.4	0.8	0.3
A_8	3.4	3.3	3.4
Objective function (lb)	969.0108	537.73	530.35
Number of function evaluations		4975	6375

optimization results from the classical gradient based method are added in Table 5 for verification. As shown in Table 5, the optimal weights of RSA and SA are close to those of the gradient based optimization method (Haug and Arora, 1979).

The number of function evaluations in the optimization using RSA is reduced 18.94% in continuous variable optimization, and 21.96% in discrete variable optimization in comparison to SA. In the continuous optimization shown in Table 5, the optimal weight from RSA is 2.9% less than SA. In the discrete optimization shown in Table 6, the optimal weight from RSA is 1.3% larger than the optimal weight from SA. The optimization by RSA requires a smaller number of iterations and produces close optimization results in comparison to SA.

4. Conclusions

In this paper, RSA has been introduced to reduce computational efforts in SA. The truss structures with both continuous and discrete design variables have been optimized using RSA and SA. Objective functions are structural weights and design variables are cross sectional areas of truss members. Constraints are allowable stresses in members and allowable displacement at joints. The continuous optimization results have been compared for the verification of the present work to the results from the classical gradient optimization method. The present optimization results are close to the previous works. Optimization results of RSA and SA have been compared to each other. The optimization results of RSA are somewhat better than the results of SA. The function evaluation numbers of RSA are smaller than SA. The function evaluations have been reduced by RSA. It is shown that RSA is well applied to the optimization of truss structures and can be extended to the optimization of general structures.

Acknowledgment

This work was performed for the Smart

Unmaned Aerial Vehicles Development Program Center, one of 21st Century Frontier R&D Programs funded by the Ministry of Science and Technology of Korea.

References

Aarts, E. and Kost, J., 1989, Simulated Annealing and Boltzmann Machines, John Wily & Sons Inc.

Aarts, E. and van Laarhoven, P., 1987, Simulated Annealing : Theory and Applications, Kluwer Academic Publishers.

Balling, R. J., 1991, "Optimal Steel Frame Design by Simulated Annealing," *Journal of Structural Engineering*, Vol. 117, pp. 1780~1795.

Bennage, W. A. and Dhingra, A. K., 1995, "Single and Multi Objective Structural Optimization in Discrete-Continuous Variables using Simulated Annealing," *International Journal for Numerical Methods in Engineering*, Vol. 38, pp. 2753~2773.

Černy, V., 1985, "Thermodynamical Approach to the Traveling Salesman Problem : An Efficient Simulated Algorithm," *Journal of Optimization Theory and Applications*, Vol. 45, No. 1, pp. 41~51.

Cui, G. Y. and Tai, K., 2000, and Wang, Topology Optimization for Maximum Natural Frequency using Simulated Annealing and Morphological Representation, 41st AIAA Structures, Structural Dynamics and Materials Conference and Exhibit, Atlanta, GA, AIAA-2000-1393.

Gelatt, C. D., Kirkpatrick, S. and Vecchi, M. P., 1983, Optimization by Simulated Annealing, Science 220, pp. 671~680.

Haug, E. J. and Arora, J. S., 1979, Applied Optimal Design, Wiley-Interscience Publication.

Herault, L., 2000, "Rescaled Simulated Annealing-Accelerating Convergence of Simulated Annealing by Rescaling the States Energies," *Journal of Heuristics*, Vol. 6, No. 2, pp. 215~252.

Ingber, L., 1995, "Adaptive Simulated Annealing : Lessons Learned," *Journal of Control and Cybernetics*, Vol. 25, No. 1.

Kincaid, R. K. and Padula, S. L., 1990, Minimizing Distortion and Internal Forces in Truss Structures by Simulated Annealing, AIAA 1095-CP.

Lundy, M., 1986, Convergence of an Annealing Algorithm, Mathematical Programming, Vol. 34, pp. 111~124.

Park, J. S. and Song, S. B., 2002, "Optimization of a Composite Laminated Structure by Network-based Genetic Algorithm," *KSME International Journal*, Vol. 16, No. 8, pp. 1033~1038.

Rao, S. S., 1996, Engineering Optimization Theory and Practice, 3rd Ed., John Wily & Sons Inc.